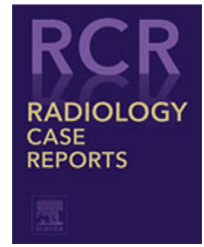


Available online at www.sciencedirect.com

ScienceDirect

journal homepage: www.elsevier.com/locate/radcr

Case Report

Epithelioid hemangioendothelioma of spine: A case report with review of literatures [☆]

Ping-Kang Chen, MS^a, Qi-Ting Lin, MS^a, You-Zhen Feng, MS^a, Ze-Ping Weng, MS^b, Xiang-Ran Cai, MD^{a,*}

^aMedical Imaging Center, First Affiliated Hospital of Jinan University, No.613 West Huangpu Avenue, Tianhe District, Guangzhou 510630, Guangdong, China

^bDepartment of Pathology, First Affiliated Hospital, Jinan University, Guangzhou, Guangdong, China

ARTICLE INFO

Article history:

Received 18 August 2020

Revised 10 October 2020

Accepted 10 October 2020

Keywords:

Epithelioid hemangioendothelioma

Spine

Magnetic resonance imaging

Positron emission computed

tomography

ABSTRACT

Primary epithelioid hemangioendothelioma of the spine is the extremely rare malignant vascular neoplasm with an unpredictable outcome. A case of epithelioid hemangioendothelioma with multiple lytic lesions of thoracolumbar spine and other bones in a 29-year-old male patient is reported. A review of the published data regarding this rare neoplasm is also presented. The features of epithelioid hemangioendothelioma include the occurrence in the young male patient, multiple osteolytic lesions with thin sclerotic rim and hypermetabolic activities. However, its imaging features are not specific. Positron emission tomography/computed tomography is essential for identification of the lesions and subsequent follow-up for treatment.

© 2020 Published by Elsevier Inc. on behalf of University of Washington.

This is an open access article under the CC BY-NC-ND license

(<http://creativecommons.org/licenses/by-nc-nd/4.0/>)

Background

Epithelioid hemangioendothelioma (EHE) is a rare vascular tumor with the most common sites such as liver, lung, and bones. It was described for the first time in 1975 by Dail and Liebow as an aggressive bronchoalveolar cell carcinoma [1]. According to 2020 WHO Classification of Bone Tumors, the bone EHE is defined as a low- to intermediate-grade malignant neoplasm. EHE of bone can involve the long tubular bones of the extremity, the axial skeleton, and the phalanges of the hand and foot [2]. However, most of them were published as

a case report because of its low prevalence. Also, EHE can be easily misdiagnosed as a multiple myeloma, metastatic tumor and so on due to the nonspecific clinical and imaging features in clinical practice. Here we report a 29-year-old male case with the complete data, including clinical, imaging (X-ray, computed tomography [CT], ¹⁸F-fluorodeoxyglucose positron emission tomography/computed tomography [¹⁸F-FDG-PET/CT]), and magnetic resonance imaging [MRI]), surgical, histopathological information, and the adjuvant therapy following the surgery. In addition, the literatures of bone EHE

[☆] Competing interests: none.

* Corresponding author.

E-mail addresses: 729594144@qq.com (P.-K. Chen), 303548393@qq.com (Q.-T. Lin), fengyouzhen@jnu.edu.cn (Y.-Z. Feng), wengzping@163.com (Z.-P. Weng), caixran@jnu.edu.cn (X.-R. Cai).

<https://doi.org/10.1016/j.radcr.2020.10.024>

1930-0433/© 2020 Published by Elsevier Inc. on behalf of University of Washington. This is an open access article under the CC BY-NC-ND license (<http://creativecommons.org/licenses/by-nc-nd/4.0/>)



Fig. 1 – Epithelioid hemangioendothelioma in the T9 vertebral body appeared as the heterogeneous signal on the preoperative T1-weighted (A) and T2-weighted (B and C) images.



Fig. 2 – Multifocal lesions were noted in L3 and L5 vertebral bodies on the preoperative T1-weighted (A) and T2-weighted (B, C, and D) images. The narrowing spinal canal was caused by the mass in L3 and the right margin of tumor (A and B) demonstrated prominently expansive growth and compressed the right psoas major muscle and caused water retention within it (C and D).

were reviewed as well. The aim of this study is to summarize its clinical and imaging features in order to guide the correct diagnosis and treatment.

Case report

A 29-year-old male patient was admitted to our hospital because of chronic low back pain for 5 months, which had been worsening for 2 months with the numbness in the right lower limb. When he bended down and turned around, the low back pain became more prominent, but the function of gait and sphincter were unaffected. No obvious tenderness was observed and the muscle force and strength of his 4 limbs were normal. He had no history of trauma.

Thoracolumbar MRI displayed the multifocal osteolytic lesions with soft tissue mass and peritumoral edema involving the vertebral bodies of T9, L3, and L5. The mass was heterogeneously isohyperintense to muscle on T1-weighted imaging and hyperintense on T2-weighted imaging (Figure 1 and 2). The presence of high signal intensity on T1-weighted imaging may represent hemorrhage. Heterogeneous enhancement

was seen on postcontrast T1-weighted images. The spinal canal narrowing was caused by the mass in L3 (Figure 2A-C) because it involved the right vertebral pedicle and compressed the cauda equina. Also, the tumors in L3 and L5 vertebrae demonstrated the prominently expansive growth, which compressed the right psoas major muscle (Figure 2).

The CT examination clearly revealed the osteolytic lesions with a thin sclerotic rim in the vertebral bodies of C1, T9, L3, L5, right inferior pubic ramus and left ilium (Figure 3A-F). ¹⁸F-FDG-PET/CT scan showed multiple hypermetabolic activities with the maximal standardized uptake value (SUV) of 5.1 in the involved bones. Most of these hypermetabolic regions corresponded well with the lytic areas on the CT images (Figure 4A-F).

The patient subsequently underwent the partial resection of tumor, L3 laminectomy, and posterior instrumentation with pedicle screws from L2 to S1. The mass had a gray-white and gray-brown color, round or lobulated shape, well-defined boundary, smooth surface and firm texture. In histopathological analysis, the epithelioid cells arranged in the glandular pattern with the clear cytoplasm, and no obvious cell atypia was found (Figure 5A-B). In immunohistochemistry analysis, the neoplastic cells were positive for CD31,

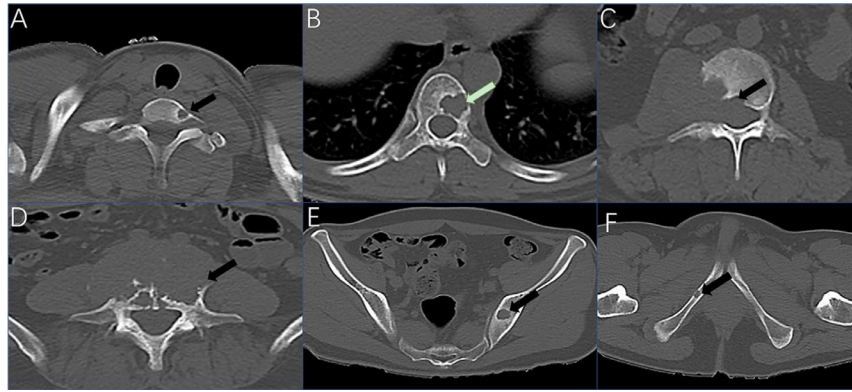


Fig. 3 – The CT examination clearly revealed the more osteolytic lesions with a thin sclerotic rim in the vertebral bodies of C1 (A), T9 (B), L3(C), L5(D), left ilium (E), and right inferior pubic ramus (F).

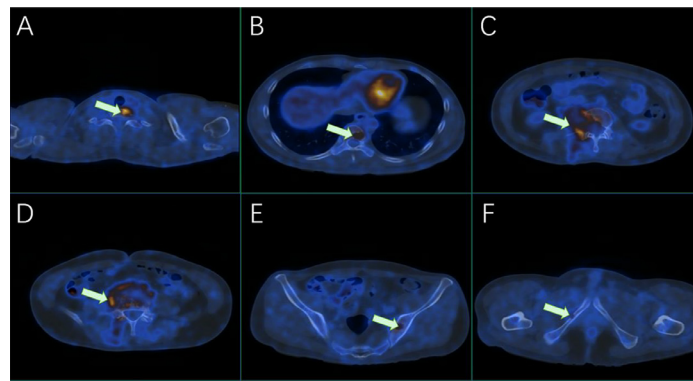


Fig. 4 – ^{18}F -FDG-PET/CT scan showed multiple hypermetabolic activities with the maximal standardized uptake value (SUV) of 5.1 in the C1 (A), T9 (B), L3 (C), L5 (D), left ilium (E), and right inferior pubic ramus (F). Most of these hypermetabolic regions corresponded well to the lytic areas on the CT images.

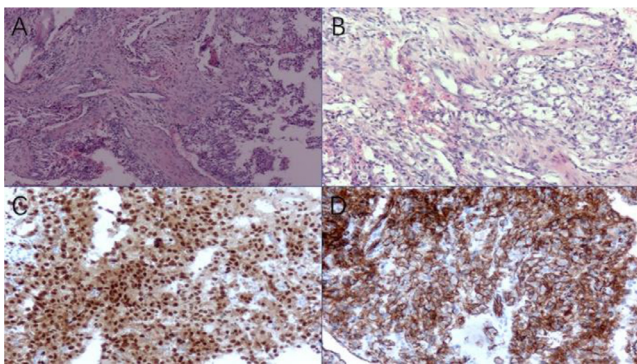


Fig. 5 – The lesions showed spindle-shaped tumor cells and epithelioid tumor cells arranged in nests or vascular lumens (A; hematoxylin and eosin, $\times 50$); The higher magnification of expanded sinusoids lined by large epithelioid tumor cells (B; hematoxylin and eosin, $\times 100$); Tumor cells were positive for the endothelial marker, ERG (C; ERG immunostaining, $\times 100$); Tumor cells were positive for the endothelial marker, CD31 (D; CD31 immunostaining, $\times 100$).

ERG, and vimentin (Figure 5C-D). Thus, the diagnosis of EHE was confirmed. Postoperative twenty courses of radiotherapy (D95PTV:5300cGy/26F) and 6 courses of chemotherapy (Paclitaxel Liposome with Avanstin) were then administered to the patient.

At about 1 week after surgery, the X-ray showed the lumbar laminectomy and posterior fusion with rods, screws, and crosslinks in the reconstruction of the spinal stability in the patient (Figure 6). Three months after surgery, the MRI and ^{18}F -FDG-PET/CT examinations revealed the masses at L3 and L5 vertebrae kept stable (Figure 7-8 and 9E-F). However, the left lateral margin of T9 vertebra was destroyed by the enlarged mass. Also, a new small lesion was found in the vertebral body of L1. After 7 months of surgical treatment, ^{18}F -FDG-PET/CT scan displayed new hypermetabolic activities in the clavicle (Figure 9A, upper arrow; B, upper arrow), scapula (Figure 9A, lower arrow), sternum (Figure 9D), sacral (Figure 9G), and other thoracic vertebrae (Figure 9B, lower arrow; C) with the maximal SUV of 5.4. Until April of 2019, the patient remained the regular radiological and clinical follow-up. He was in a stable situation without the low back pain and the numbness of arms and legs.

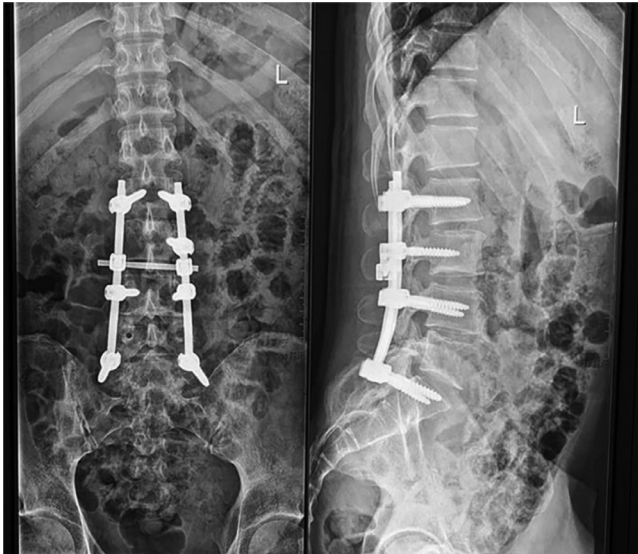


Fig. 6 – Postoperative X-ray scan showed the partial resection of tumor, L3 laminectomy, and posterior instrumentation with pedicle screws from L2 to S1.



Fig. 7 – Postoperative MRI scan revealed the mass at L3 and L5 (A and B) vertebral bodies kept stable.



Fig. 8 – Postoperative MRI scan revealed the mass at L3 and L5 (A and B) vertebral bodies kept stable.

Discussion

Arising from endothelial or preendothelial cells, EHE is a rare malignant vascular mass [3]. Its most common presenting symptom is pain, which may be associated with a mass. The neurological symptoms depend on the location of the mass [4,5]. EHE of bone may occur at any age with the predilection age between 20 and 30 years. It is more prevalent in males and male-to-female ratio is 2:1 [6]. But Kerry et al. [5] reported that the men and women were affected in roughly equal numbers as well. According to Weissferdt et al. [7], the overall survival for those EHE patients with unicentric tumor was 89% compared with 50% in patients with multifocal diseases. And metastatic disease was present in up to 30% of cases and the mortality rate was about 20%. In addition, a median survival was 1.3 years after disease progression and the 5-year survival was approximately 33% [8].

Macroscopically, EHE usually appears as a reddish-brown loculated mass with significant hemorrhage and the light red or purple surface. The formation of multicellular infantile angiogenic sprouts and lumens are noted in the tumor [5,9]. The distinct well-lined anastomosing vascular channels often seen in hemangiopericytoma are absent in this tumor [5]. Microscopically, the tumor cells are round, polygonal or fusiform with a central nucleus, and prominent intracytoplasmic vacuolation [10]. Blood lacunae are seen in the cytoplasm of individual cells. Tumor cells are arranged in cords and nests, which are embedded within a myxohyaline stroma. In immunohistochemistry, the positivity of endothelial cell markers CD34, CD31, and factor VIII-related antigen is specific for the diagnosis of EHE [5].

Multifocal lesions or metastasis of bone EHE are frequently seen. Some cases showed the multicentric lesions within a bone [12,13], while other cases exhibited the multifocal changes within the multiple bones, randomly distributed throughout the skeleton or clustered in an anatomic region, such as a single extremity [5,14]. The clear distinction between the multifocal and metastatic disease does not exist. A recent study of liver EHE revealed the monoclonal origin of multifocal EHE by demonstrating identical breakpoint rearrangements of WWTR1-CAMTA1 fusion genes, indicating the metastatic implants of the same neoplastic clone [14].

Multimodality imaging plays a critical role in the assessment and management of patients with EHE. But the low prevalence and variable presentation of EHE often makes it misdiagnosed [15]. On X-ray or CT scan, the typical characteristic of bone EHE is an osteolytic lesion with well-defined margin and without matrix mineralization [5,16,17]. On MRI, it also shows the lytic lesion with a sclerotic rim [2]. But the signal intensity of the tumor is nonspecific, such as the low-to-intermediate signal intensity in T1-weighted images, high signal or high-hybrid intensity on T2-weighted images, and restricted diffusion. A halo sign could be found around the lesion after administration of contrast medium, representing visible enhancement at the inner edge, and gradually toward the center [2,15,17]. The characteristics of aggression or metastasis of EHE could make the radiologists to conclude the wrong diagnosis of osteomyelitis or other malignancy [10]. In our case, the EHE was found in the multiple vertebrae and other bones

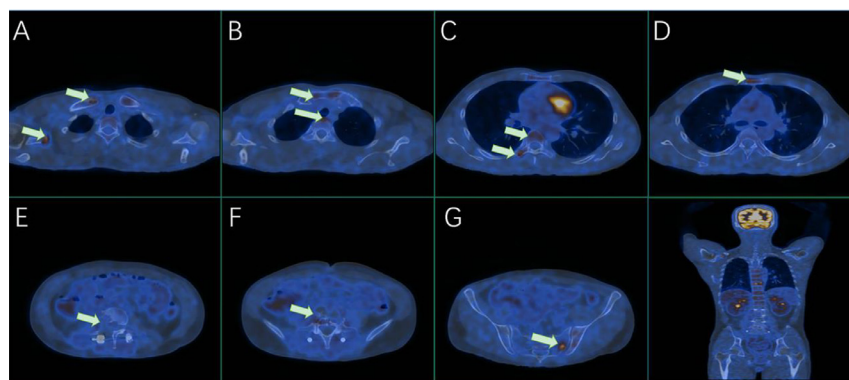


Fig. 9 – Postoperative ^{18}F -FDG-PET/CT scan showed more new hypermetabolic activities in the scapula (A), clavicle (A and B), sternum (D), sacral (G), and other thoracic vertebrae (B, lower arrow; C) with the maximal-standardized uptake value of 5.4, but the mass at L3 (E) and L5 (F) vertebral bodies kept stable.

throughout the body with the expansive and osteolytic lesions. And the adjacent soft tissue was affected as well.

In recent years, ^{18}F -FDG-PET/CT is considered to be a promising tool for the diagnosis and evaluation of primary malignant tumor. The increased FDG uptake in EHE of bone and soft tissue was reported [18–20]. A higher SUV value was found in the nidus of pelvic and lower limbs [18,21,22] and the lower SUV value was shown in spinal EHE by Ozguven et al. [23] and our case. Also, the greater SUV value was noticed in the male cases [18,21]. To prove these tendencies, more EHE cases with PET/CT are needed for further analysis. The PET/CT images showed the multiple regions of intensely increased FDG uptake activity and most of these regions corresponded well with the osteolytic lesions [18,21,23]. Thus, the metastasis or metabolic bone disease is often suspected. The PET/CT study of our case showed the multiple skeletal lesions with hypermetabolic activity throughout the body which was in accordance to the lytic lesions on CT scan. Our case indicate that the ^{18}F -FDG-PET/CT could play an important role in detecting and depicting EHE lesions, especially for multiple lesions.

Multifocal EHE of bone can be easily misdiagnosed as the metastases. Also, it should be distinguished from epithelioid hemangioma and angiosarcoma. Differentiation for them is difficult because of the overlapping imaging features. However, the histopathology will be helpful for differentiation [11]. The presence of cord-like arrangement or characteristic stroma helps distinguish EHE from epithelioid hemangioma. And angiosarcoma lacks the typical myxohyaline stroma and WWTR1-CAMTA1 fusion genes of EHE.

There is still no standard treatment guideline because of the rarity of spinal EHE and its unpredictable natural course. Treatment approaches for spinal EHE include surgical treatment, radiotherapy, and chemotherapy. Kerry et al. [5] and Albakr et al. [24] believed that the most common treatment for spinal EHE was the surgical resection combined with adjuvant radiation therapy. Luzzati et al. [25] reported that those patients, who had undergone wide or marginal resection, had a better prognosis. Sebastian et al. [26] described that a novel multimodal treatment, consisting of a partial L2 corpectomy, tumor resection, bone grafting, and vertebral reconstruction using a minimally invasive technique, could

reduce the morbidity compared to traditional techniques. The patient was pain-free without further progression or regression of the tumor and signs of instability at his follow-up 3.5 years after surgery [26]. Radiotherapy is recommended to reduce the risk of local recurrence after surgery [10,27]. Kerry et al. [5] reported a 17-year-old male patient, undergoing a combination treatment including subtotal tumor resection, radiation therapy, and chemotherapy, was asymptomatic during an 11-year follow-up period. The patient in our case was in a stable condition without pain during the 7-month follow-up after a combination treatment. However, more new lesions were found in other bones.

Conclusion

In summary, our case appears as the typical features of multifocal EHE, including the occurrence in the young male patient, osteolytic lesions with thin sclerotic rim involving the multiple bones. However, its imaging features are not specific. It is worthy of reminding the radiologists to keep it in mind as a differential diagnosis in cases of multifocal lesions of bone in the young patient. In addition, considering its multifocal feature, PET/CT is essential for identification of the lesions and subsequent follow-up for treatment.

Patient consent statement

We already have the consent from the patient before we submit the case report.

REFERENCES

- [1] Lee YJ, Chung MJ, Jeong KC, Hahn CH, Hong KP, Kim YJ, et al. Pleural epithelioid hemangioendothelioma. *Yonsei Med J* 2008;49(6):1036–40.

- [2] Epelboym Y, Engelkemier DR, Thomas-Chausse F, Alomari AI, Al-Ibraheemi A, Trenor CC, et al. Imaging findings in epithelioid hemangioendothelioma. *Clin Imaging* 2019;58:59–65.
- [3] Läufer JM, Zimmermann A, Krähenbühl L, Triller J, Baer HU. Epithelioid hemangioendothelioma of the liver. A rare hepatic tumor. *Cancer* 1996;78(11):2318–27.
- [4] Lau K, Massad M, Pollak C, Rubin C, Yeh J, Wang J, et al. Clinical patterns and outcome in epithelioid hemangioendothelioma with or without pulmonary involvement: insights from an internet registry in the study of a rare cancer. *Chest* 2011;140(5):1312–18.
- [5] Kerry G, Marx O, Kraus D, Vogel M, Kaiser A, Ruedinger C, et al. Multifocal epithelioid hemangioendothelioma derived from the spine region: case report and literature review. *Case Rep Oncol* 2012;5(1):91–8.
- [6] Ignacio EA, Palmer KM, Mathur SC, Schwartz AM, Olan WJ. Epithelioid hemangioendothelioma of the lower extremity. *Radiographics* 1999;19(2):531–7.
- [7] Weissferdt A, Moran CA. Epithelioid hemangioendothelioma of the bone: a review and update. *Adv Anat Pathol* 2014;21(4):254–9.
- [8] Gómez-Arellano LI, Ferrari-Carballo T, Domínguez-Malagón HR. Multicentric epithelioid hemangioendothelioma of bone. Report of a case with radiologic-pathologic correlation. *Ann Diagn Pathol* 2012;16(1):43–7.
- [9] Wang CG, Jia NY, Yu HY, Liu HM, Wang J. Epithelioid hemangioendothelioma of thoracic vertebra: a case report (2008: 11b). *Eur Radiol* 2009;19(2):517–20.
- [10] Kelahan LC, Sandhu FA, Sayah A. Multifocal hemangioendothelioma of the lumbar spine and response to surgical resection and radiation. *Spine J* 2015;15(11):e49–e56.
- [11] O'Shea BM, Kim J. Epithelioid hemangioma of the spine: two cases. *Radiol Case Rep* 2014;9(4):984.
- [12] Zhang H, Fu Y, Ye Z. Bone multicentric epithelioid hemangioendothelioma of the lower and upper extremities with pulmonary metastases: a case report. *Oncol Lett* 2015;9(5):2177–80.
- [13] Liu Q, Miao J, Lian K, Huang L, Ding Z. Multicentric epithelioid hemangioendothelioma involving the same lower extremity: a case report and review of literature. *Int J Med Sci* 2011;8(7):558–63.
- [14] Errani C, Sung YS, Zhang L, Healey JH, Antonescu CR. Monoclonality of multifocal epithelioid hemangioendothelioma of the liver by analysis of WWTR1-CAMTA1 breakpoints. *Cancer Genet* 2012;205(1-2):12–17.
- [15] Zeng Y, Leng X, Chen P, Luo J, Zhou Z. Imaging diagnosis of epithelioid hemangioendothelioma in thoracic vertebrae and liver. *Ann Thorac Surg* 2020;109(6):e407–ee10.
- [16] Xu Y, Chen W, Cheng H, Lin Z. Epithelioid hemangioendothelioma of the bone: a case report with findings of bone scintigraphy. *Medicine (Baltimore)* 2019;98(19):e15546.
- [17] Adler B, Naheedy J, Yeager N, Nicol K, Klamar J. Multifocal epithelioid hemangioendothelioma in a 16-year-old boy. *Pediatr Radiol* 2005;35(10):1014–18.
- [18] Rao M, Chen Y, Huang Z, Zhu Y, Xiao X. FDG PET/CT findings of multifocal epithelioid hemangioendotheliomas of the bones. *Clin Nucl Med* 2015;40(10):821–2.
- [19] Albano D, Bosio G, Tironi A, Bertagna F. (18)F-FDG PET/CT in pleural epithelioid hemangioendothelioma. *Asia Oceania J Nucl Med Biol* 2017;5(1):70–4.
- [20] Ergün EL, Lim E. Increased FDG uptake in pulmonary epithelioid hemangioendothelioma. *Rev Esp Med Nucl* 2006;25(3):188–92.
- [21] Zhao H, Han J, Qin L, Zhang C. Primary left tibial epithelioid hemangioendotheliomas with multiple metastases revealed by FDG PET/CT imaging. *Clin Nucl Med* 2016;41(11):872–3.
- [22] Treglia G, Ceriani L, Paone G, Rusca T, Bongiovanni M, Giovannella L. Multifocal epithelioid hemangioendothelioma of the lower limbs detected by 18F-FDG PET/MRI. *Clin Nucl Med* 2014;39(9):e402–e4e4.
- [23] Ozguven S, Kesim S, Oksuzoglu K, Dane F, Ones T, Erdil TY. (18)F-FDG PET/CT findings of a rare case of diffuse hepatic epithelioid hemangioendothelioma with bone metastases at diagnosis. *Rev Esp Med Nucl Imagen Mol* 2020;39(1):39–40.
- [24] Albakr A, Schell M, Drew B, Cenic A. Epithelioid hemangioendothelioma of the spine: case report and review of the literature. *J Spine Surg* 2017;3(2):250–9.
- [25] Luzzati A, Gagliano F, Perrucchini G, Scotto G, Zoccali C. Epithelioid hemangioendothelioma of the spine: results at seven years of average follow-up in a series of 10 cases surgically treated and a review of literature. *Eur Spine J* 2015;24(10):2156–64.
- [26] Sebastian AS, Adair MJ, Morris JM, Khan MH, Arndt CA, Nassr A. Minimally invasive treatment of a painful osteolytic lumbar lesion secondary to epithelioid hemangioendothelioma. *Global Spine J* 2015;5(2):135–9.
- [27] Campanacci M, Boriani S, Giunti A. Hemangioendothelioma of bone: a study of 29 cases. *Cancer* 1980;46(4):804–14.